



Published in final edited form as:

Am J Surg Pathol. 2015 May ; 39(5): 581–591. doi:10.1097/PAS.0000000000000387.

Clinical, Histopathologic and Genomic Features of Spitz Tumors with ALK Fusions

Iwei Yeh, MD, PhD¹, Arnaud de la Fouchardiere, MD, PhD², Daniel Pissaloux, PhD², Thaddeus W. Mully, MD¹, Maria C. Garrido, MD, PhD¹, Swapna S. Vemula, MS¹, Klaus J. Busam, MD³, Philip E. LeBoit, MD¹, Timothy H. McCalmont, MD¹, and Boris C. Bastian, MD, PhD¹

¹Department of Dermatology and Pathology, University of California, San Francisco

²Department of Biopathologie, Centre Leon Berard

³Department of Pathology, Memorial Sloan Kettering Cancer Center

Abstract

Activating kinase fusions have recently been described as early oncogenic events that are mutually exclusive with HRAS and BRAF mutations in Spitz tumors. Here, we report a series of 32 Spitz tumors with ALK fusions (6 Spitz nevi, 22 atypical Spitz tumors, and 4 Spitzoid melanomas) in patients ranging from 5 months to 64 years (median=12 y) of age. The tumors typically presented as exophytic papules on the extremities and were occasionally darkly pigmented. In addition to ALK fusions previously described in other tumor types (NPM1-ALK, TPR-ALK) we identified 2 novel ALK fusions (CLIP1-ALK and GTF3C2-ALK) in our cohort of Spitz tumors. Array comparative genomic hybridization of 19 of these tumors demonstrated a high frequency of chromosome 2 aberrations (where ALK resides, 63%) and chromosome 1p loss in 37% of the cases. Spitz tumors with ALK fusions demonstrated unique histopathologic features. Clefts and small vesicle-like spaces were arrayed between plump spindled melanocytes with fibrillar cytoplasm and enlarged nuclei. These melanocytes were typically arrayed in elongated and fusiform nests with radial orientation. The tumors often had extension into the dermis or subcutis with a wedge-shaped or bulbous lower border (45% and 17% respectively). An infiltrative growth pattern was often present at the periphery of the tumor and was highlighted by ALK immunohistochemistry. In conclusion, Spitz tumors with ALK rearrangement show distinct histopathologic features that should aid in improving classification of these diagnostically challenging tumors.

Introduction

Spitz tumors are subgroup of melanocytic neoplasms with distinctive histopathological features such as increased cell size and epithelioid or spindled morphology. They are more common in children and adolescents, but can occur at all ages. The histopathologic diagnosis of Spitz tumors is notoriously difficult. While polar examples can be reliably

recognized histopathologically, there are many intermediate grade lesions in which there is a small but real risk of widespread metastasis. Cases on the benign end of the spectrum with no overlapping morphologic features with melanoma are designated as Spitz nevi, whereas cases with unequivocal features of melanoma are designated as Spitzoid melanomas. Borderline cases that show overlapping features of Spitz nevus and melanoma have been termed atypical Spitz tumors.

The genetic landscape of Spitz tumors is unfolding and the differences compared to other categories of melanocytic neoplasms are emerging rapidly¹. Spitz tumors generally have no mutations in BRAF, NRAS, or KIT, the most commonly activated oncogenes in melanocytic neoplasms with an intraepithelial component nor mutations in GNAQ or GNA11, which are primarily found in melanocytic neoplasms without epithelial involvement such as blue nevi and related lesions, melanocytomas and uveal melanomas¹. One notable exception is the setting of bi-allelic loss of BAP1, which, in the presence of a BRAF^{V600E} mutation leads to a distinctive neoplasm with large epithelioid melanocytes reminiscent of Spitz nevus². In contrast to classical Spitz nevi the neoplasms with BRAF^{V600E} mutations and loss of BAP1 lack the epidermal hyperplasia typical of Spitz nevi and their epithelioid melanocytes do not usually form junctional nests^{2,3}.

Previous studies revealed that approximately 20% of Spitz nevi harbor activating mutations of HRAS, often accompanied by gain of the mutant HRAS allele via copy number increases of the entire short arm of chromosome 11⁴. Spitz nevi with these genetic alterations display distinctive features, frequently presenting as mostly dermal based lesions with a horizontal rather than vertical orientation, often with marked desmoplasia^{4,5}. Recently we reported that Spitz tumors without mutations in HRAS or BRAF frequently have genomic rearrangements that lead to fusions involving the threonine kinase BRAF (in its wild-type form) or the receptor tyrosine kinases ALK, ROS1, NTRK1, and RET^{6,7}. The fusion kinases are formed by intra- or interchromosomal rearrangements that result in chimeric genes in which the 3' portion of the kinase gene is linked to the 5' portion of another gene to give rise to an in-frame mRNA transcript that encodes a chimeric protein with a constitutively activated kinase. The expression of the fusion transcript is driven by the promoter of the 5' partner, decoupling the regulation of expression of the fusion kinase from regulation of the corresponding wild-type kinase. Some of the kinases such as ALK, ROS1 and RET, are not expressed in most adult cells including melanocytes, and the expression of the activated kinase is considered a pivotal oncogenic event in multiple different tumor types such as anaplastic large cell lymphoma (ALK), inflammatory myofibroblastic tumor (ALK), non-small cell lung cancer (ALK, ROS1, RET)⁸, and thyroid cancer (RET, NTRK1)^{9,10}. While there is overlap in the 5' partners found in Spitz tumors with those found in other neoplasms, multiple novel 5' fusion partners have been identified in Spitz tumors^{6,7}. Kinase fusions in Spitz tumors were found throughout the entire spectrum of the disease from unequivocally benign Spitz nevi to Spitzoid melanomas, indicating that the fusions represent initiating oncogenic alterations, similar to BRAF, NRAS, GNAQ and GNA11, which are also found in benign nevi.

The findings point to significant genetic diversity in Spitz tumors with a range of different oncogenic driver genes, which themselves are subject to additional variation depending on

the 5' partner to which they are fused. In contrast to conventional nevi in which an activating BRAF mutation is the oncogenic driver in ~90% of cases^{11,12}, Spitz tumors are thus highly genetically heterogeneous. This indicates that part of the difficulty in developing accurate and reproducible diagnostic and prognostic parameters for Spitz tumors may be due to their genetic heterogeneity. Spitz tumors with HRAS mutation or BRAF mutation with concomitant loss of BAP1 have unique characteristics. Here we describe the morphologic and genetic features of Spitz tumors with ALK fusions as another possibly distinct subset with characteristic histopathologic features.

Material and Methods

Case selection

Spitz tumors with ALK fusion were identified during the diagnostic workup of cases reviewed at the Dermatopathology Section of the University of California, San Francisco and from Department of Biopathology at the Centre Léon Bérard in Lyon, France. The study was approved by the Committee on Human Research and was conducted according to the Declaration of Helsinki. Criteria that prompted the suspicion of an ALK rearrangement were morphological features identified in the index cases in the initial discovery cohort⁷ or copy number transitions involving the ALK locus identified by comparative genomic hybridization for clinical purposes. ALK rearrangements were confirmed by fluorescence *in situ* hybridization (FISH), next-generation sequencing including the ALK coding region and intron 19, and/or immunohistochemistry using antibodies directed at the kinase domain of ALK (UCSF: rabbit polyclonal, 1:200, Invitrogen 18-0266 (Life Technologies, Grand Island, NY), Lyon: clone 5A4, 1:100, Leica Microsystems PA0306 (Leica Microsystems, Buffalo Grove, IL). The histopathological features were assessed by two pathologists (I.Y. and A.F.).

DNA extraction

Routinely sections were used to guide microdissection. Small amounts of tumor were obtained from ten to twenty unstained 8–20 µm formalin fixed paraffin embedded (FFPE) sections. DNA extraction was performed using deparaffinization solution (Qiagen #19093, Sussex, UK) and the QIAamp® DNA FFPE Tissue Kit (Qiagen #56404, Sussex, UK) or as described previously¹³.

Array comparative genomic hybridization

Array comparative genomic hybridization (CGH) was carried out with 1–1.5 µg of genomic DNA on Agilent 4×180K microarrays (Agilent, Santa Clara, CA, USA) according to the manufacturer's instructions. Commercially available normal human DNA (Promega #G1471 or #G1521, WI, USA) was used as a reference. Scanned images were processed using Agilent Feature Extraction software. Analysis was performed with Nexus Copy Number Software version 7.0 (Biodiscovery, El Segundo, CA, USA).

Fluorescence *In Situ* Hybridization

FISH was performed on 4 µm sections of formalin-fixed paraffin-embedded tissue, using the ZytoLight FISH-Tissue Implementation Kit (Zytovision # Z-2028-20, Bremerhaven,

Germany) and the ZytoLight SPEC ALK Dual Color Break Apart Probe (ZytoVision # Z-2124-200, Bremerhaven, Germany) or the Vysis LSI ALK Break Apart Rearrangement Probe Kit (Abbott Molecular, Des Plaines, IL) as per manufacturer's instructions. FISH signals were enumerated in at least 50 non-overlapping intact nuclei. A specimen was considered positive if more than 20% of nuclei demonstrated a signal pattern consistent with an ALK rearrangement (split of orange and green signals or single orange signals without a corresponding green signal).

Targeted DNA Sequencing

For each tissue, 200ng of DNA was prepared for sequencing using the NuGen Ovation (12 samples, p/n 0331-32, San Carlos, CA) library preparation kits following the manufacturer's instructions. Capture was performed using custom Nimblegen SeqCap EZ Choice Libraries (p/n 06588786001, Madison, WI) (Table S1 for baits). Case 19 was sequenced with version 1 capture library, and cases 11, 29 and 31 were sequenced with version 2 capture library. Bar-coded samples were sequenced on an Illumina HiSeq 2500. FASTQ files were aligned using Burrows-Wheeler Aligner (BWA)¹⁴. Deduplication and assessment of coverage and sequencing statistics were performed using Picard¹⁵. INDEL realignment, recalibration, and variant calling was performed using the Genome Analysis Tool-Kit (GATK) and Unified Genotyper¹⁶. Structural rearrangements were called using CREST on informative reads (those with soft-clipping and discordant mate-pairs)¹⁷.

The target genes were curated to comprise common cancer genes with particular relevance to melanoma. For all sequenced cases, the targeted regions included the exons of ALK, BRAF, NRAS, HRAS, KRAS, GNAQ, GNA11, KIT as well as intron 19 of ALK.

Results

Clinical Findings

A total of 32 cases were included in this study, and their clinical features are summarized in Table 1. The median age of the patients was 12 years with a range from 5 months to 64 years. There was a predominance of females over male (21 and 11, binomial exact test, p-value=0.03). Eighteen (56%) of lesions arose on the extremities, 8 (25%) on the trunk, and 6 (19%) on the head and neck region. Many of the tumors were clinically amelanotic (n=12) or vascular appearing (n=3) and the clinical differential diagnosis included keloid, molluscum contagiosum, basal cell carcinoma and pyogenic granuloma (Fig. 1A). Occasionally, pigmentation was noted on clinical examination (n=5) and some tumors were black in color (Fig 1B). Seven of the tumors were 1 cm in size or larger. The final histopathologic diagnosis was Spitz nevus in 6 (19%) cases, atypical Spitz tumor in 22 cases (69%), and Spitzoid melanoma in 4 cases (12%). Spitzoid melanomas were distinguished from atypical Spitz tumors by histopathologic features including increased nuclear pleomorphism, the presence of epidermal consumption, lack of maturation, nodularity at the base of the lesion and deep mitoses. Sentinel node biopsy was negative in all 3 cases in which it was performed. Clinical follow-up was available for 20 patients and ranged from 3–40 months (median 9 months). No patient had a recurrence.

Genetic Findings

The FISH analyses (n= 17) showed three different patterns. A single hybridization signal of the probe targeting the kinase domain side of the breakpoint with a loss of the other signal was seen in 3 cases (Figure 2A). This pattern is expected to occur in rearrangements resulting from deletions such as the one that produces the DCTN1-ALK fusion, as well as other unbalanced rearrangements. Split signals were observed in 12 cases (Figure 2B), and are compatible with rearrangements resulting from a reciprocal translocation. Amplification of ALK by FISH (> 5 ALK signals per cell) was found in 2 cases (Figure 2C).

Array CGH was performed for 19 cases (Figure 3). Five cases (26%) had no detectable copy number aberration. Three cases (16%) demonstrated nearly identical interstitial deletions on the short arm of chromosome 2 (less than 0.4 Mb between start and end sites of the three deletions) suggesting a DCTN1-ALK fusion (cases 9, 25, 27). Copy number on chromosome 2 (on which ALK resides) was aberrant in most cases (n=12, 63%) with 8 of these cases demonstrating copy number aberrations on other chromosomes as well. Seven (37%) cases demonstrated loss on chromosome 1p.

ALK copy number status was assessed by either CGH or FISH for 28 cases. Gain of ALK was observed in 1 (4%) and amplification was observed in 3 (11%) cases where amplification was defined as \log_2 copy number ratio > 1.5 (CGH) or > 5 signals/cell (FISH) (Table 1). Copy number transitions within ALK with relative gain of the 3' end (encoding the kinase domain) were present in 8 (29%) cases.

In four cases, an activating ALK fusion was identified by targeted sequencing. The fusion partners of ALK identified by sequencing were NPM1, TPR, GTF3C2, and CLIP1 (Table 3). NPM1-ALK arose from reciprocal translocation, with fusion junctions for both NPM1-ALK and ALK-NPM1 identified. The other ALK fusions did not arise from reciprocal translocation. In case 11, a GTF3C2-ALK fusion with the 5' untranslated region of GTF3C2 fused to exon 18 of ALK was identified (Fig. 3). The predicted fusion transcript would utilize a cryptic translation start site within exon 18 to express the kinase domain of ALK. FISH demonstrated multiple signals (>5/cell) corresponding to the 3' end of ALK scattered throughout the nucleus (Fig. 3B). By CGH, the ~2Mb region between GTF3C2 and ALK was amplified (\log_2 ratio > 1.5), consistent with double minute formation followed by amplification (Fig. 3C). Expression of the kinase domain of ALK was confirmed by immunohistochemistry. None of cases with ALK fusions that underwent targeted sequencing had oncogenic mutations in BRAF, NRAS, HRAS, or KIT or any other oncogenes.

Histopathologic findings

The histopathologic features of the ALK fused tumors differed from those of classical Spitz nevi and are summarized in Table 2. The median tumor thickness was 2.7 mm (range 0.75–7.1 mm) and 5 tumors (16%) were ulcerated. Most lesions (78%) were compound in nature, with both an epidermal and dermal component. Of the 29 cases in which the base of the tumor was sampled, about a third (38%) demonstrated a flat base, with a majority having a wedge-shaped or bulbous (45 and 17% respectively) base. Most tumors were exophytic with

epidermal hyperplasia. Rarely, consumption of the epidermis (16%)¹⁸ was observed. Kamino bodies were also infrequent (13%). The majority of cases (91%) showed a fascicular growth pattern with melanocytes streaming in large confluent nests or sheets often oriented in a radial pattern, converging towards the base of the tumor. Large nests were often present within an edematous papillary dermis with thinning of the overlying epidermis. Most lesions were amelanotic, but focal pigmentation was present in a quarter of cases. The majority showed a pronounced infiltrative growth pattern with deep dermal invasion. Select cases that highlight these architectural features are presented in Figure 5.

ALK immunohistochemistry was strongly and homogeneously positive in 28 of 29 cases analyzed. The remaining case demonstrated intense punctate cytoplasmic staining. The pronounced infiltrative pattern is best appreciated with ALK immunohistochemistry (Fig. 6). In several cases, small clusters of ALK positive cells were seen at considerable distance from the main tumor, often with a distinctive growth pattern with narrow, pseudo-tubular strands at the periphery of the tumor (Fig. 6A). Invasion of adnexal structures was noted in a majority of the cases, with melanocytes observed within arrector pili, eccrine ducts, and follicular epithelium (Figure 6B).

Most of the tumors demonstrated fusiform to polygonal melanocytes with clefts or small vesicle-like spaces separating neighboring cells (Fig. 7). Their cytoplasm was amphophilic with a fibrillar quality. In many cases the melanocytes had enlarged nuclei and prominent nucleoli (Fig. 7B). When pigment was noted in melanocytes, it had a coarsely granular quality (Fig. 7B). Multinucleated melanocytes were present in over one-third of cases. Dermal mitoses were not uncommon, observed in almost half (47%) the tumors.

Discussion

The term Spitz tumor is used to describe melanocytic tumors with a predominance of large epithelioid or spindled melanocytes across a spectrum from benign to malignant¹. These tumors are often diagnostically challenging because they display features associated with melanoma such as large melanocytes with abundant cytoplasm and large nuclei, mitotic figures, and deep dermal involvement. While they commonly involve local lymph nodes, distant metastasis is infrequent^{19,20}. The development of distinct diagnostic criteria for Spitz nevi, separate from those used for common or conventional nevi, greatly improved the accuracy of classification of these tumors. Even with the recognition that Spitz tumors have unique histopathologic features, there is often disagreement among expert dermatopathologists as to their biologic potential^{21,22}.

The genetic diversity of Spitz tumors may explain the difficulty in developing reliable and reproducible diagnostic criteria for these tumors. ALK fusions are estimated to be present in ~ 8% of Spitz nevi, ~5% of Atypical Spitz tumors, and ~1% of Spitzoid melanomas⁷. In this study, we present Spitz tumors with ALK fusions as a distinct subset of Spitz tumors that can be distinguished by genetic features, immunohistochemistry, and histopathology. The age distribution of our patients was broad (5 months to 64 years), but the majority of tumors occurred in children, similar to what has been previously observed for Spitz nevi and atypical Spitz tumors. None of the patients' tumors recurred, including the 4 patients with

spitzoid melanoma who were each followed for more than 1 year. While no Spitz tumors with ALK fusions are yet reported to have widely disseminated, it is important to note that kinase inhibitors targeting ALK are approved for clinical use in other cancers driven by these fusions.

The ALK fused tumors in our study demonstrated some distinctive histopathologic features. We found that ALK fused tumors were often exophytic and composed of large nests of fusiform melanocytes arranged in elongated and radially vertically oriented nests, similar to prior studies^{7,23}. ALK fused tumors often demonstrated a wedge-shaped or bulbous base and adnexal extension and a markedly infiltrative growth pattern at the lateral and deep periphery of the tumors, best appreciated by ALK immunohistochemistry. A minority of the tumors contained melanocytes with coarsely granular pigment, and melanocytes with dusty melanin pigmentation (so-called pulverocytes) that have been noted in Spitzoid melanomas were not present²⁴. As in other neoplasms with ALK rearrangements, ALK immunohistochemistry with an antibody against the kinase domain of ALK accurately reflected the genetic findings. These features were present in tumors ranging from benign to malignant.

Our study expands the range of ALK fusions documented in Spitz tumors. Previous studies identified DCTN1 and TPM3 as recurrent N-terminal fusion partners of ALK in Spitz tumors^{7,23}. In the four cases we sequenced, we identified ALK fusions not previously described in Spitz tumors. An NPM1-ALK fusion resulted from a t(2;5) translocation; this translocation is found in a majority of anaplastic large cell lymphomas²⁵. A similar TPR-ALK fusion to that which we identified was recently described in lung adenocarcinoma²⁶. The identification of a CLIP1-ALK fusion supports the hypothesis that the N-terminal partners of kinase fusions may be interchangeable within Spitz tumors as CLIP1 also partners with ROS1 in Spitz tumors⁷. GTF3C2, a subunit of transcription factor IIIc, has not been previously reported to participate in oncogenic fusions. The GTF3C2-ALK fusion we identified appeared to be the result of double minute formation. Copy number aberrations on chromosome 2 (where ALK is located) were present in most of the tumors, and this finding is uncommon in prior CGH studies of Spitz nevi and tumors²⁷⁻³⁰. Seven (37%) cases demonstrated loss on chromosome 1p, an aberration not previously reported to occur at significant frequency in Spitz nevi, or atypical Spitz tumors, or melanoma.

While ours is the largest cohort of ALK fused Spitz tumors assembled to date, additional studies are necessary to refine these criteria and determine whether the biological behavior of these lesions is different from other emerging subtypes of Spitz tumors. If confirmed, dividing Spitz tumors into subtypes defined by a combination of genetic, histopathological and clinical features is likely to improve the accuracy of diagnosing these lesions in the future.

Supplementary Material

Refer to Web version on PubMed Central for supplementary material.

Acknowledgments

We thank the dermatopathologists who shared these cases in consultation with us and provided follow-up information. We thank the technical staff of Centre Leon Berard's Biopathology lab especially Amandine Bernard. We thank Emmanuelle Bourrat for providing a clinical picture. Dr. Yeh is supported by a grant from the Dermatology Foundation. Dr. Bastian is supported by a grant from the NIH/NCI (P01 CA025874).

References

1. Bastian BC. The Molecular Pathology of Melanoma: An Integrated Taxonomy of Melanocytic Neoplasia. *Annu Rev Pathol Mech Dis.* 2014; 9:239–271.10.1146/annurev-pathol-012513-104658
2. Wiesner T, Murali R, Fried I, et al. A Distinct Subset of Atypical Spitz Tumors is Characterized by BRAF Mutation and Loss of BAP1 Expression. *Am J Surg Pathol.* 2012;10.1097/PAS.0b013e3182498be5.
3. Yeh I, Mully TW, Wiesner T, et al. Ambiguous Melanocytic Tumors With Loss of 3p21. *Am J Surg Pathol.* 2014;10.1097/PAS.0000000000000209.
4. Bastian BC, LeBoit PE, Pinkel D. Mutations and Copy Number Increase of HRAS in Spitz Nevi with Distinctive Histopathological Features. *Am J Pathol.* 2000; 157:967–972.10.1016/S0002-9440(10)64609-3 [PubMed: 10980135]
5. Van Engen-van Grunsven ACH, van Dijk MCRF, Ruiter DJ, et al. HRAS-mutated Spitz tumors: A subtype of Spitz tumors with distinct features. *Am J Surg Pathol.* 2010; 34:1436–1441.10.1097/PAS.0b013e3181f0a749 [PubMed: 20871217]
6. Botton T, Yeh I, Nelson T, et al. Recurrent BRAF kinase fusions in melanocytic tumors offer an opportunity for targeted therapy. *Pigment Cell Melanoma Res.* 2013;10.1111/pcmr.12148.
7. Wiesner T, He J, Yelensky R, et al. Kinase fusions are frequent in Spitz tumours and spitzoid melanomas. *Nat Commun.* 2014;5.10.1038/ncomms4116.
8. Takeuchi K, Soda M, Togashi Y, et al. RET, ROS1 and ALK fusions in lung cancer. *Nat Med.* 2012; 18:378–381.10.1038/nm.2658 [PubMed: 22327623]
9. Klugbauer S, Demidchik EP, Lengfelder E, et al. Detection of a Novel Type of RET Rearrangement (PTC5) in Thyroid Carcinomas after Chernobyl and Analysis of the Involved RET-fused Gene RFG5. *Cancer Res.* 1998; 58:198–203. [PubMed: 9443391]
10. Rabes HM, Demidchik EP, Sidorow JD, et al. Pattern of radiation-induced RET and NTRK1 rearrangements in 191 post-chernobyl papillary thyroid carcinomas: biological, phenotypic, and clinical implications. *Clin Cancer Res Off J Am Assoc Cancer Res.* 2000; 6:1093–1103.
11. Pollock PM, Harper UL, Hansen KS, et al. High frequency of BRAF mutations in nevi. *Nat Genet.* 2003; 33:19–20.10.1038/ng1054 [PubMed: 12447372]
12. Yeh I, von Deimling A, Bastian BC. Clonal BRAF mutations in melanocytic nevi and initiating role of BRAF in melanocytic neoplasia. *J Natl Cancer Inst.* 2013; 105:917–919.10.1093/jnci/djt119 [PubMed: 23690527]
13. Bastian BC, LeBoit PE, Hamm H, et al. Chromosomal gains and losses in primary cutaneous melanomas detected by comparative genomic hybridization. *Cancer Res.* 1998; 58:2170–2175. [PubMed: 9605762]
14. Li H, Durbin R. Fast and accurate short read alignment with Burrows-Wheeler transform. *Bioinforma Oxf Engl.* 2009; 25:1754–1760.10.1093/bioinformatics/btp324
15. Broad Institute. Picard. Available at: <http://broadinstitute.github.io/picard/>
16. DePristo MA, Banks E, Poplin R, et al. A framework for variation discovery and genotyping using next-generation DNA sequencing data. *Nat Genet.* 2011; 43:491–498.10.1038/ng.806 [PubMed: 21478889]
17. Wang J, Mullighan CG, Easton J, et al. CREST maps somatic structural variation in cancer genomes with base-pair resolution. *Nat Methods.* 2011; 8:652–654.10.1038/nmeth.1628 [PubMed: 21666668]
18. Hantschke M, Bastian BC, LeBoit PE. Consumption of the epidermis: a diagnostic criterion for the differential diagnosis of melanoma and Spitz nevus. *Am J Surg Pathol.* 2004; 28:1621–1625. [PubMed: 15577682]

19. Busam KJ, Murali R, Pulitzer M, et al. Atypical spitzoid melanocytic tumors with positive sentinel lymph nodes in children and teenagers, and comparison with histologically unambiguous and lethal melanomas. *Am J Surg Pathol*. 2009; 33:1386–1395.10.1097/PAS.0b013e3181ac1927 [PubMed: 19609204]
20. Ludgate MW, Fullen DR, Lee J, et al. The atypical Spitz tumor of uncertain biologic potential: a series of 67 patients from a single institution. *Cancer*. 2009; 115:631–641.10.1002/cncr.24047 [PubMed: 19123453]
21. Barnhill RL, Argenyi ZB, From L, et al. Atypical Spitz nevi/tumors: lack of consensus for diagnosis, discrimination from melanoma, and prediction of outcome. *Hum Pathol*. 1999; 30:513–520. [PubMed: 10333219]
22. Gerami P, Busam K, Cochran A, et al. Histomorphologic assessment and interobserver diagnostic reproducibility of atypical spitzoid melanocytic neoplasms with long-term follow-up. *Am J Surg Pathol*. 2014; 38:934–940.10.1097/PAS.000000000000198 [PubMed: 24618612]
23. Busam KJ, Kutzner H, Cerroni L, et al. Clinical and Pathologic Findings of Spitz Nevi and Atypical Spitz Tumors With ALK Fusions. *J Surg Pathol*. Jul.2014 38:925–933.10.1097/PAS.0000000000000187
24. Massi, Guido L.; Emanuel, Philip. *Histological Diagnosis of Nevi and Melanoma*. Springer; 2014. Histological diagnosis of nevi and melanoma; p. 502-503.
25. Morris SW, Kirstein MN, Valentine MB, et al. Fusion of a kinase gene, ALK, to a nucleolar protein gene, NPM, in non-Hodgkin's lymphoma. *Science*. 1994; 263:1281–1284. [PubMed: 8122112]
26. Choi Y-L, Lira ME, Hong M, et al. A novel fusion of TPR and ALK in lung adenocarcinoma. *J Thorac Oncol Off Publ Int Assoc Study Lung Cancer*. 2014; 9:563–566.10.1097/JTO.0000000000000093
27. Bastian BC, Wesselmann U, Pinkel D, et al. Molecular cytogenetic analysis of Spitz nevi shows clear differences to melanoma. *J Invest Dermatol*. 1999; 113:1065–1069.10.1046/j.1523-1747.1999.00787.x [PubMed: 10594753]
28. Harvell JD, Kohler S, Zhu S, et al. High-resolution array-based comparative genomic hybridization for distinguishing paraffin-embedded Spitz nevi and melanomas. *Diagn Mol Pathol Am J Surg Pathol Part B*. 2004; 13:22–25.
29. Ali L, Helm T, Cheney R, et al. Correlating array comparative genomic hybridization findings with histology and outcome in spitzoid melanocytic neoplasms. *Int J Clin Exp Pathol*. 2010; 3:593–599. [PubMed: 20661407]
30. Raskin L, Ludgate M, Iyer RK, et al. Copy number variations and clinical outcome in atypical spitz tumors. *Am J Surg Pathol*. 2011; 35:243–252.10.1097/PAS.0b013e31820393ee [PubMed: 21263245]

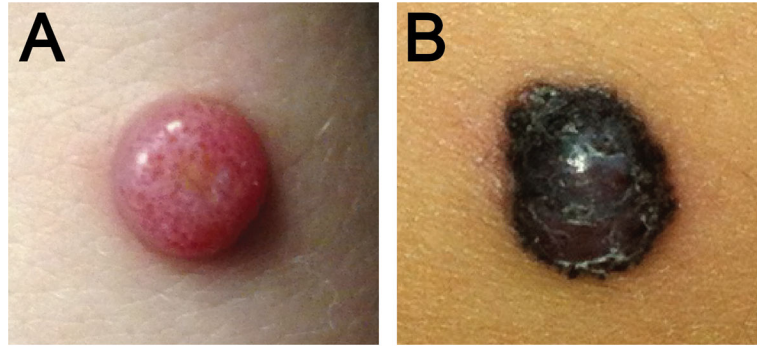


Figure 1. Clinical Appearance of Atypical Spitz Tumors with ALK fusion

A. Amelanotic 1.2 cm exophytic nodule on the distal forearm of a 17 year old woman (Case 3). **B.** Pigmented, irregularly bordered papule of 5.5 mm diameter, rapidly growing on the thigh of a 4 year old girl undergoing maintenance treatment for B-cell acute lymphoblastic leukemia (Case 10).

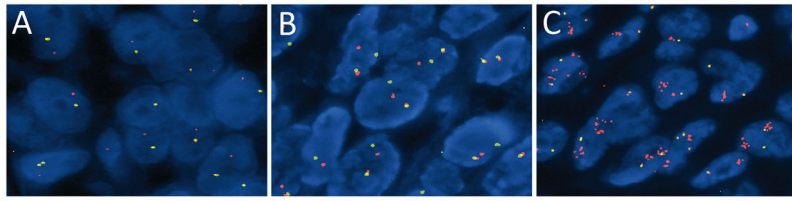


Figure 2. Disruption of ALK identified by FISH A

Unbalanced rearrangement of the ALK gene, with preservation of the 3' signal (red) and the remaining intact ALK gene (1 juxtapsed green and orange signal). **B.** Balanced rearrangement of the ALK gene with separated orange and green signals compared to the remaining intact locus. **C.** Amplification of the 3' oncogenic signal (1 or 2 fusion signals + numerous clustered orange signals).

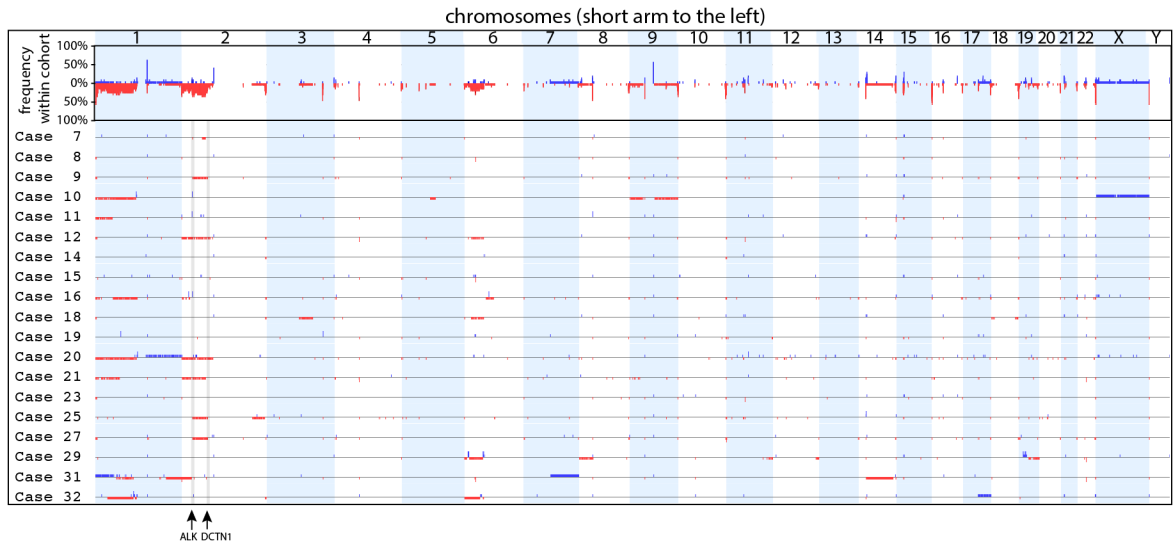


Figure 3. Overview of CGH results

The top panel shows the frequency of copy number changes at each genomic position of the entire cohort indicating recurrent losses of chromosomes 1p, 2p and 6p. The rows below show the individual cases along the same axis. Red regions below the axis represent areas of loss. Blue regions above the axis represent areas of gain. Amplifications defined by regions with a \log_2 ratio > 1.5 are shown as areas with a higher blue block. The genomic positions of ALK and DCTN1 are noted at the bottom. Cases 9, 25, and 27 demonstrate deletion of the region of 2p between ALK and DCTN1 suggestive of a DCTN1-ALK fusion.

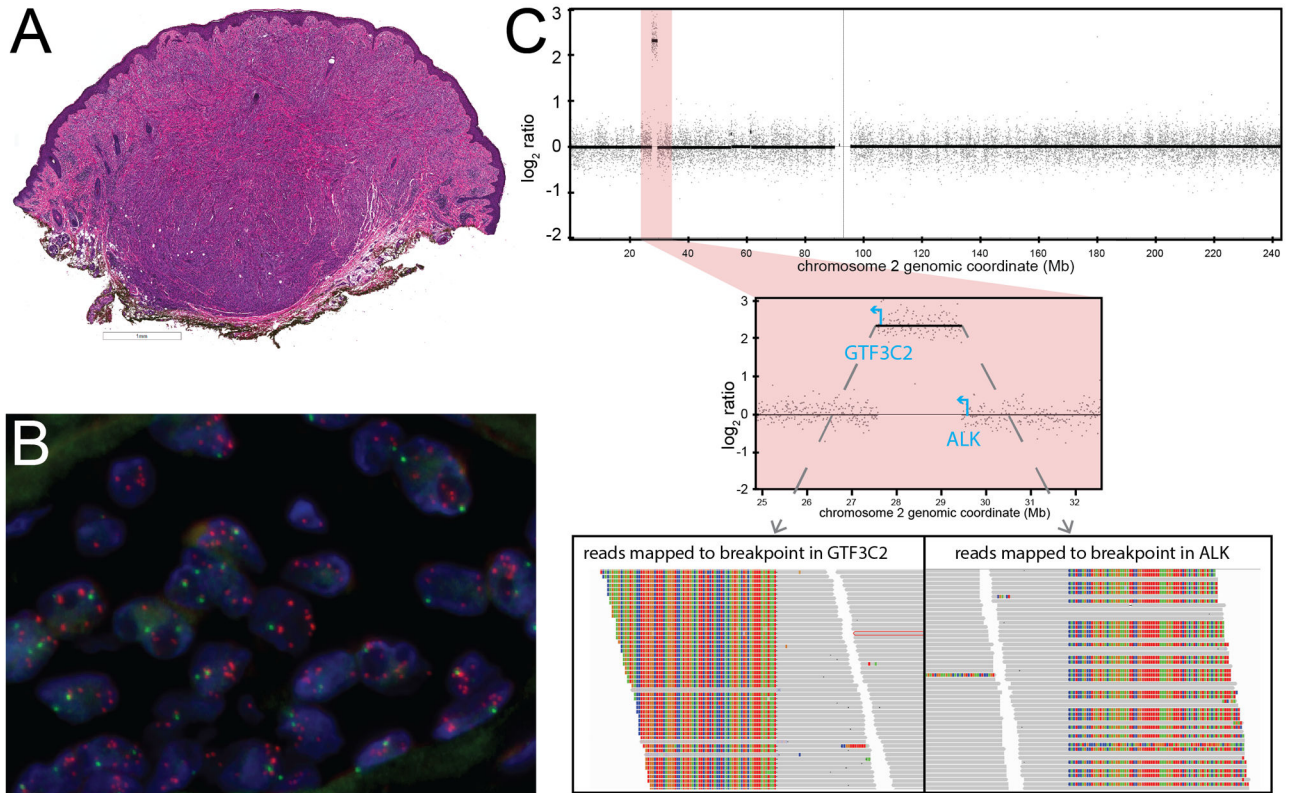


Figure 4. Atypical Spitz tumor with GTF3C2-ALK fusion arising from double minute formation
A. Low-power view demonstrates a dome-shaped, predominantly intradermal melanocytic tumor with a bulbous base. **B.** FISH demonstrates multiple signals for the probe targeting the 3' end of ALK (orange) scattered within the nuclei of melanocytes. **C.** Log₂ ratio along chromosome 2 obtained by CGH demonstrates a focal amplification (top). The amplicon is ~2 Mb long and is flanked by GTF3C2 and ALK (center). Reads that map to the breakpoints in GTF3C2 and ALK demonstrate unaligned regions that flank the breakpoint (rainbow colored, as viewed in Integrative Genomics Viewer).

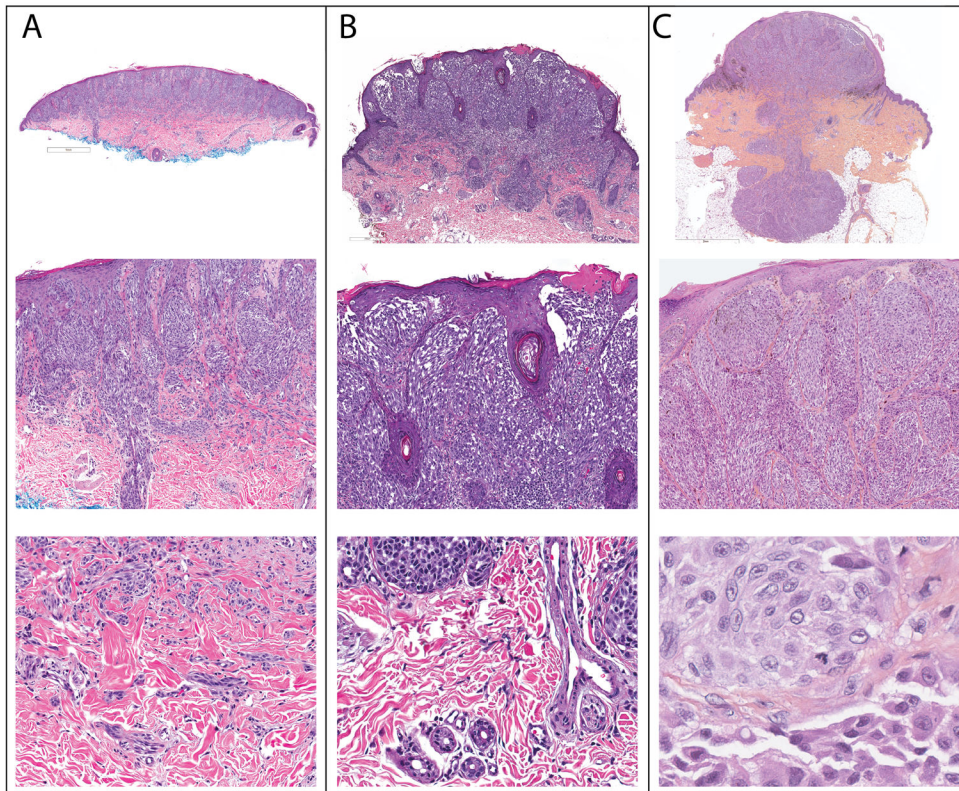


Figure 5. Architectural features of ALK fused Spitz tumors

A. Case 23. A dome-shaped tumor with a flat base (top). There is overlying epidermal hyperplasia with vertically oriented fascicles of melanocytes in the superficial portion of the tumor. Melanocytes extend along an eccrine duct (middle). At the base, melanocytes infiltrate between collagen bundles. **B. Case 19.** Exophytic tumor with a wedge shaped base (top). Thin elongated rete ridges are present with focal ulceration above radially and vertically oriented fascicles of melanocytes (middle). Single melanocytes are present between collagen bundles at the base (bottom). **C. Case 10.** Exophytic tumor in “dumb-bell” configuration with a bulbous base extending into the subcutis (top). Large fascicles of fusiform melanocytes are present in the papillary dermis below thinned suprapapillary plates (middle). Mitotic figures are present in the deep portion of the tumor (bottom).

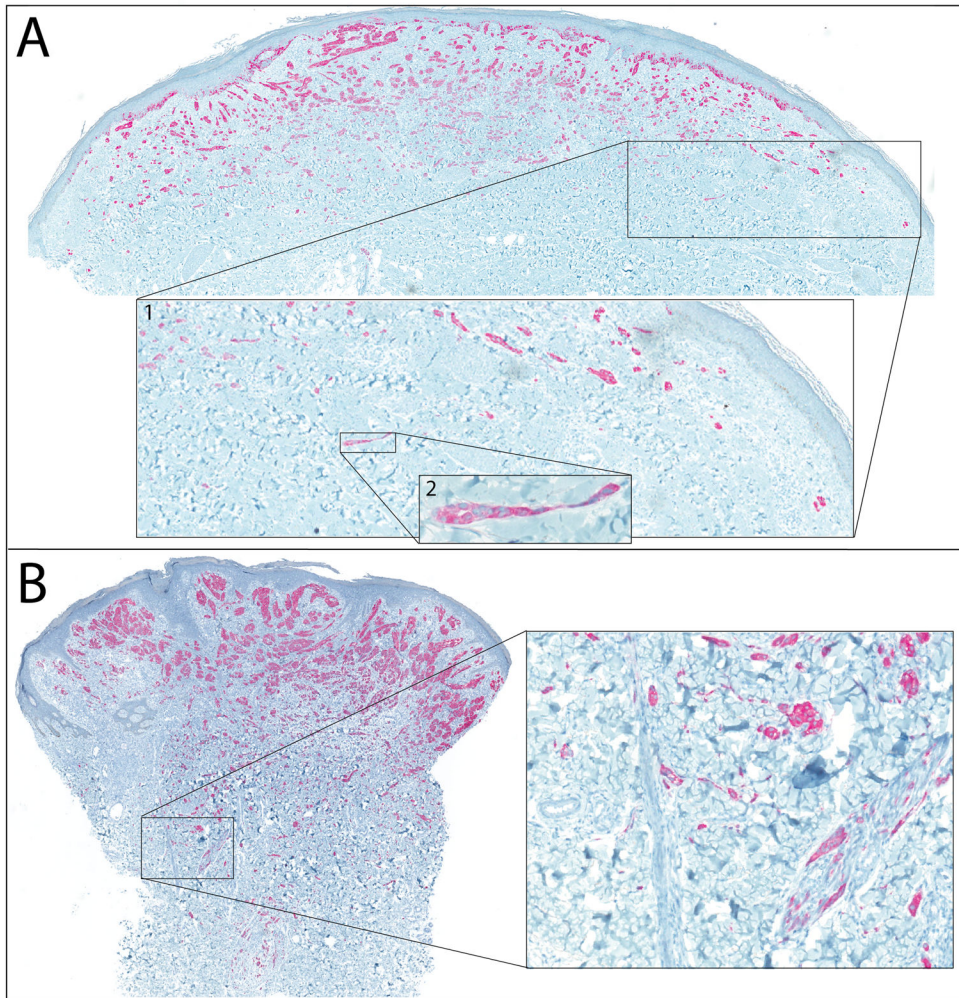


Figure 6. ALK immunohistochemistry highlights infiltrative growth pattern

A. Case 28. Neoplastic melanocytes are strongly positive for ALK by

immunohistochemistry. Inset 1 shows small clusters of melanocytes at a distance from other collections of melanocytes. Inset 2 shows the pseudoglandular configuration of one of these collections of melanocytes at the periphery of the tumor. **B. Case 26.** Invasion of ALK-

positive melanocytes into the deep dermis. Inset shows single cells between collagen bundles at the base of the tumor and nests of melanocytes within arrector pili.

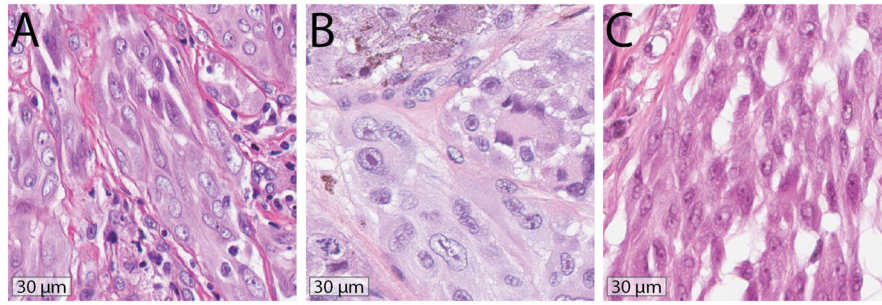


Figure 7. Distinct Cytologic Features In ALK Fused Spitz Tumors

A. Case 2. Fusiform melanocytes contain amphiphilic cytoplasm with a fibrillar quality. Clefts and rounded spaces are present between melanocytes. **B. Case 10.** Increased nuclear size and prominent nucleoli are present. Some melanocytes demonstrate cytoplasmic pigment, others are multinucleated. The cytoplasm has a faintly fibrillar quality and small rounded spaces are present between adjacent melanocytes. A mitotic figure is present. **C. Case 17.** Clefting is present between fusiform melanocytes.

Table 1

Features of ALK fused Spitz tumors.

Case	Age (yrs)	Gender	Location	Final Diagnosis [#]	Clinical History	Clinical follow-up	Copy number transition in ALK	Gain or Amplification of ALK fusion *	Studies performed
1	4	F	arm	Spitz nevus	0.5 cm lesion	NED 3 months	No	No	FISH, IHC
2	15	M	knee	Spitz nevus	0.7 mm verrucous papule	Re-excision, NED 9 months	No	No	FISH, IHC
3	17	F	wrist	Spitz nevus	1.2 cm exophytic pink nodule	Re-excision, lost to follow-up	NA	NA	IHC
4	24	F	lower back	Spitz nevus	1.3 cm oval, growing, pink lesion, basal cell carcinoma?	NED 9 months	FISH	No	FISH, IHC
5	31	M	back	Spitz nevus	pink papule, in prior radiation field for Hodgkin's lymphoma	lost to follow-up	NA	NA	IHC
6	39	F	buttock	Spitz nevus	irritated Spitz	lost to follow-up	No	No	FISH, IHC
7	0.4	F	forearm	atypical Spitz tumor	pyogenic granuloma/hemangioma	Re-excision, NED 3 months	CGH	No	CGH, IHC
8	3	M	cheek	atypical Spitz tumor	xanthogranuloma versus nevus versus molluscum	Re-excision, lost to follow-up	No	No	CGH, IHC
9	4	F	cheek	atypical Spitz tumor	1.5 cm pink plaque with border of pigmentation and cobblestone texture	Re-excision, lost to follow-up	CGH	No	CGH, IHC
10	4	F	thigh	atypical Spitz tumor	5.5 mm papule, rapid growth noted while on maintenance treatment for B-cell acute lymphoblastic leukemia	Re-excision, NED 9 months	CGH, FISH	AMP (CGH/FISH)	CGH, FISH, IHC
11	5	F	ear	atypical Spitz tumor	recently enlarging	Re-excision, lost to follow-up	CGH	AMP (CGH/FISH)	CGH, FISH, IHC Seq
12	5	M	knee	atypical Spitz tumor	ulcerated 0.6 cm pink papule	lost to follow-up	CGH, FISH	No	CGH, FISH, IHC
13	5	F	elbow	atypical Spitz tumor	growing 0.5 cm exophytic pink papule	Re-excision, lost to follow-up	No	No	FISH, IHC
14	6	M	leg	atypical Spitz tumor	pink nodule	lost to follow-up	No	No	CGH, FISH, IHC
15	7	F	scalp	atypical Spitz tumor	rapidly growing pink and black papule	Re-excision, NED 3 months	No	No	CGH, IHC
16	7	F	lower leg	atypical Spitz tumor	Unavailable	Re-excision, NED 4 months	No	AMP (CGH)	CGH, IHC

Case	Age (yrs)	Gender	Location	Final Diagnosis [#]	Clinical History	Clinical follow-up	Copy number transition in ALK	Gain or Amplification of ALK fusion*	Studies performed
17	7	M	forearm	atypical Spitz tumor	pyogenic granuloma	Re-excision, NED 9 months	No	No	FISH, IHC
18	7	F	forearm	atypical Spitz tumor	1.5 cm infiltrative nodule	Re-excision, NED 9 months	No	No	CGH, FISH, IHC
19	9	F	cheek	atypical Spitz tumor	not available	Re-excision, NED 7 months	No	No	CGH, Seq
20	11	M	chest	atypical Spitz tumor	Spitz nevus	Re-excision, lost to follow-up	CGH	GAIN (CGH)	CGH, IHC
21	13	F	arm	atypical Spitz tumor	keloid	Re-excision, NED 3 months	No	No	CGH, IHC
22	16	F	ear	atypical Spitz tumor	1 cm exophytic, pink papule	Re-excision, NED 12 months	No	No	FISH, IHC
23	17	F	buttock	atypical Spitz tumor	1 cm pink plaque	Re-excision, NED 8 months	No	No	CGH, IHC
24	17	M	hand	atypical Spitz tumor	1 cm exophytic, pink, nodule	Re-excision, NED 9 months	No	No	FISH, IHC
25	18	F	lower abdomen	atypical Spitz tumor	not available	Re-excision, SLNBx -, NED 4months	CGH	No	CGH, IHC
26	21	M	forearm	atypical Spitz tumor	0.6 cm lesion	Re-excision, lost to follow up	No	No	FISH, IHC
27	27	F	lower back	atypical Spitz tumor	angiomatous plaque with central pigmentation	Re-excision, NED 18 months	CGH	No	CGH, IHC
28	64	F	leg	atypical Spitz tumor	0.6 cm lesion	Re-excision, lost to follow-up	No	No	FISH, IHC
29	5	M	buttock	Spitzoid melanoma, > 7 mm	pyogenic granuloma	Re-excision, NED 13 months	No	No	CGH, Seq
30	13	F	forearm	Spitzoid melanoma, 7.1 mm	Inflamed pink papule	Re-excision, SLNBx - NED 40 months	No	No	FISH, IHC
31	17	F	foot	Spitzoid melanoma, 1.75 mm	traumatized melanocytic neoplasm	Re-excision, SLNBx -, NED 21 months	No	No	CGH, Seq
32	21	M	arm	Spitzoid melanoma, 3.5 mm	0.8 mm pigmented nodule	Re-excision, NED 16 months	No	No	CGH, FISH, IHC

NED: no evidence of disease SLNBx: sentinel lymph node biopsy FISH: fluorescence in situ hybridization CGH: comparative genomic hybridization IHC: immunohistochemistry

[#] Breslow depth is provided for the melanomas.

* Amplification defined as log2 copy number ratio > 1.5 (CGH) or > 5 signals/cell (FISH).

Author Manuscript

Author Manuscript

Author Manuscript

Author Manuscript

Table 2

ALK fusions identified by targeted DNA sequencing.

Case	N-terminal Fusion Partner (Transcript ID)	Genomic location	Intron of N-terminal partner rearranged	Location of rearrangement in ALK (NM_004304)	Classification of Structural Rearrangement	Reads Supporting Fusion	Average Coverage
11	GTF3C2 (NM_001521)	2p23.3	1	exon 18	double minute	760	330
19	NPM1 (NM_002520)	5q35.1	4	intron 20	reciprocal translocation	26	244
29	CLIP1 (NM_002956)	12q24.31	13	intron 20	NOS	28	205
31	TPR (NM_003292)	1q31.1	4	intron 20	complex	33	283

NOS: not otherwise specified

Table 3

Histopathologic characteristics of ALK fusion spitz tumors.

Architectural Features	Cases Observed/Evaluated (%)
Silhouette	
Exophytic	19/32(59%)
Tumor base	
Flat base	11/29(38%)
Wedge-shaped base	13/29(45%)
Bulbous base	5/29(17%)
Epidermal changes	
Epidermal hyperplasia	25/32(78%)
Epidermal consumption	5/32(16%)
Ulceration	5/32(16%)
Characteristics of Junctional Component	
Junctional nests present	25/32(78%)
Pagetoid scatter	15/32(47%)
Kamino Bodies	4/32(13%)
Architecture	
Fascicular Growth Pattern	29/32(91%)
Infiltrative pattern at periphery	21/29(72%)
Large superficial nests	19/32(59%)
Tubular/cord like growth pattern	16/29(55%)
Adnexal extension	
Eccrine gland extension	10/30(33%)
Follicular extension	9/30(30%)
Within arrector pili	9/30(30%)
Perineural extension	3/30(10%)
Any of the above	21/30(70%)
Cytologic Features	
Fibrillar cytoplasm	27/32(84%)
Large nuclei with prominent nucleoli	26/32(81%)
Rounded spaces between melanocytes	25/32(78%)
Clefts between melanocytes	21/32(66%)
Multinucleated melanocytes	12/32(38%)
Necrotic melanocytes	10/32(31%)
Cytoplasmic Pigmentation	9/32(28%)
Other	
Dermal mitoses	17/32(53%)
Permeative lymphocytic infiltrate	14/32(44%)
Melanophages in papillary dermis	12/32(38%)